

XAFS Study on Deterioration of Cathode Materials for Lithium-Ion Batteries

Takamasa Nonaka, Chikaaki Okuda, Yasuhito Kondo, Yoshiki Seno
and Yoshio Ukyo

Toyota Central R&D Labs., Inc., 41-1, Nagakute, Aichi, 480-1192, Japan

Abstract. $\text{LiNi}_{0.8}\text{Co}_{0.15}\text{Al}_{0.05}\text{O}_2$, being one of the promising cathode materials for lithium-ion batteries, shows a distinct capacity fading after charge/discharge cycling and/or storage at high temperatures. The origin of these deteriorations has been explored by investigating the electronic and structural changes of the cathode material using X-ray absorption spectroscopy. Ni K-edge XAFS measurements were performed in two different modes: surface-sensitive conversion electron yield (CEY) mode and bulk-sensitive transmission mode. The Ni K-edge XANES showed that, after the cycle and aging tests, the Ni valences at the near-surface of the cathode particles became much lower than those in bulk. Whereas, the EXAFS showed that the bulk and surface-averaged Ni-O bond distances remained unchanged after the tests. These electronic and structural changes which occur prominently at near-surface are probably the main cause of the battery deterioration phenomenon.

Keywords: Li-ion battery; Ni oxides; Conversion electron yield

PACS: 82.47.Aa

INTRODUCTION

$\text{LiNi}_{0.8}\text{Co}_{0.15}\text{Al}_{0.05}\text{O}_2$ is being considered as a promising cathode material because of its improved stability and electrochemical performance brought by Co and Al substitutions for Ni in LiNiO_2 [1]. $\text{LiNi}_{0.8}\text{Co}_{0.15}\text{Al}_{0.05}\text{O}_2$ remains as a single rhombohedral phase during charge/discharge cycling, allowing a high cycling reversibility. In spite of such improvements, $\text{LiNi}_{0.8}\text{Co}_{0.15}\text{Al}_{0.05}\text{O}_2$ still has the problem of deteriorations such as capacity fading and the increase in impedance [2]. These deteriorations occur during use (i.e., on electrochemical cycling) and/or on storage at high temperatures, being one of the most crucial problems which should be overcome for applications requiring a very long life, such as electric vehicles. Although the mechanism of deteriorations is considered to be quite complicated, we have found that, in the case of the battery using $\text{LiNi}_{0.8}\text{Co}_{0.15}\text{Al}_{0.05}\text{O}_2$, the increase in impedance is predominantly attributed to the cathode [2]. It has been also reported that, in the battery using $\text{LiNi}_{0.8}\text{Co}_{0.2}\text{O}_2$, the charge-transfer resistance at the cathode-electrolyte interface is the main cause of the impedance increase [3].

In this study, we have employed conversion electron yield (CEY) XAFS [4] at the Ni K-edge as a

tool to explore the near-surface regions of the cathode particles. Furthermore, combining CEY-XAFS with conventional XAFS in the transmission mode allows us to compare near-surface-averaged information with bulk-averaged information on cathode material particles. This combined probe has a potential to offer a new insight into the battery deterioration mechanism. The purposes of this study are (1) to clarify the changes in the oxidation state and local structure of Ni during charge/discharge for a fresh (not deteriorated) battery, and (2) to elucidate the changes induced by cycle and aging tests.

EXPERIMENTAL

The cathode sheets removed from 18650-type cells were used as samples [2]. The cell consisted of a cathode sheet, an anode sheet, an electrolyte and a separator. The cathode sheet was a thin Al foil on both sides of which ~20 μm thick electrode mixtures were coated, containing 85 wt% $\text{LiNi}_{0.8}\text{Co}_{0.15}\text{Al}_{0.05}\text{O}_2$, 10wt% conductive materials and 5wt% polyvinylidene fluoride (PVDF) binder. The $\text{LiNi}_{0.8}\text{Co}_{0.15}\text{Al}_{0.05}\text{O}_2$ cathode material comprised 10–15 μm secondary particles, each of which was composed of smaller primary particles. The cells which exhibited various levels of capacity fading were prepared: fresh cells,

cycle tested cells (1000 cycles at 60 °C) and aging tested cells (storage at 60 °C for a year). The discharge capacity of each cell condition is 160, 123 and 125 mAh/g, respectively. In order to investigate the change accompanied by charging (Li-deintercalation), the cells with various states of charge were prepared for each cell condition. The Li contents in $\text{Li}_{1-x}\text{Ni}_{0.8}\text{Co}_{0.15}\text{Al}_{0.05}\text{O}_2$ ($0.07 < x < 0.71$) were determined by inductively coupled plasma-atomic emission spectroscopy (ICP-AES).

The CEY and transmission XAFS measurements were performed on the beamline BL16B2 of the Spring-8 (Hyogo, Japan). A newly developed detector was used for the CEY-XAFS. A sample surrounded by an atmospheric pressure helium gas is irradiated with X-rays, which produces the emission of electrons (predominantly Ni KLL Auger electrons in this case) from the sample surface. Each electron induces the cascade ionization of He atoms, generating a bunch of He ions and secondary electrons. The resultant He ions and secondary electrons are collected with high-voltage biased carbon electrodes. Schroeder *et al.* has reported that the probing depth of Ni K-edge CEY-XAFS for NiO is experimentally estimated to be ~90 nm [5]. We infer from their estimation that the probing depth of the present measurement is almost the same value as theirs since the near-surface region of the $\text{Li}_{1-x}\text{Ni}_{0.8}\text{Co}_{0.15}\text{Al}_{0.05}\text{O}_2$ particles exhibits Ni-O-like properties as shown later.

RESULTS AND DISCUSSION

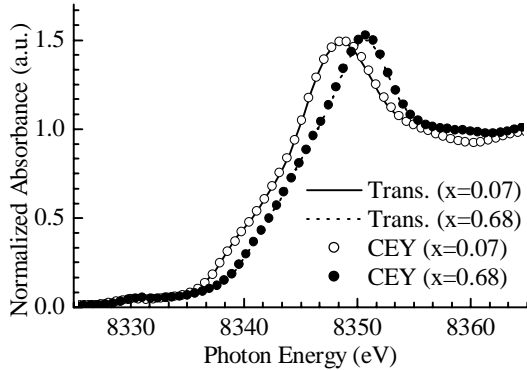


FIGURE 1. XANES spectra for $\text{Li}_{1-x}\text{Ni}_{0.8}\text{Co}_{0.15}\text{Al}_{0.05}\text{O}_2$ at the Ni K-edge obtained in transmission XAFS (Trans.) and conversion electron yield XAFS (CEY).

Figure 1 shows representative Ni K-edge XANES spectra of $\text{Li}_{1-x}\text{Ni}_{0.8}\text{Co}_{0.15}\text{Al}_{0.05}\text{O}_2$ ($x=0.07, 0.68$) obtained in both the transmission and CEY XAFS for the fresh cell. It can be seen that, in both edges, the shapes and signal-to-noise ratios of XANES spectra obtained in different techniques are completely identical. This ensures the validity of the quantitative

comparison of the results deduced from the two techniques at least in XANES region. As Li is deintercalated (x increases), the entire pattern of the Ni K-edge spectrum shifts to higher energies, indicating the oxidization of Ni atoms.

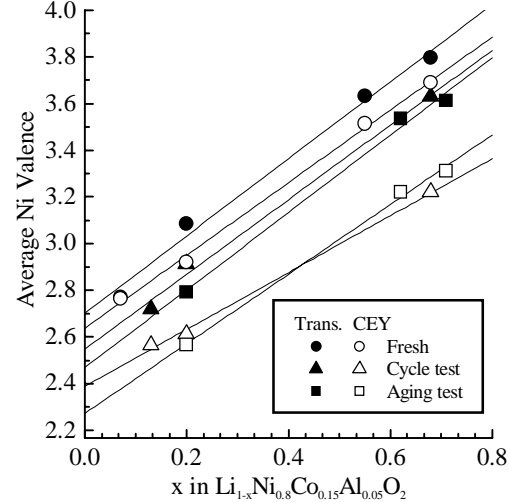


FIGURE 2. Comparison of average Ni valences estimated using the edge positions of the XANES spectra along with approximate lines.

The value of the energy at half-step height (where normalized absorbance = 0.5) was used as a measure of oxidation state. Average Ni valences were estimated using the analytical line proposed by O' Grady *et al.* They have reported systematic linear shifts in the edge energy as a function of Ni valence [6]. Figure 2 shows a comparison of estimated average Ni valences along with approximate lines obtained by using least-squares fits. The bulk averaged (Trans.) Ni valence for the fresh cell is seen to change predominantly from trivalent to tetravalent upon charging. A comparison of the line of the surface (CEY) and that of the bulk for the fresh cell shows that the surface-averaged Ni valence is lower than the bulk-averaged one throughout all values of x . This implies that the content rate of Ni^{2+} at the fresh cell surface is larger than that in bulk. As can be clearly seen, the differences between the Ni valences at the surface and those in bulk become much larger after the cycle and aging tests. Furthermore, the slopes of the approximate lines for the surface of the tested cells, particularly of the cycle tested cell, are more gradual than those for the bulk. This implies that the content rate of divalent Ni atom is increased by the cycle and aging tests especially at the cathode material surface, and then some of Ni^{2+} turn into Ni^{3+} upon charging with the other Ni^{2+} remaining divalent states. The presence of the Ni^{2+} that no longer contributes to the charge compensation of $\text{Li}_{1-x}\text{Ni}_{0.8}\text{Co}_{0.15}\text{Al}_{0.05}\text{O}_2$ explains the

lowering of the slopes of Ni oxidization. It should be also noted that the bulk-averaged Ni valences for the tested cells are evidently lower than those for the fresh cell. This indicates that the drop of Ni valence after the cell tests, which predominantly occurs at the surface, is also visible using the bulk-sensitive transmission mode XAFS.

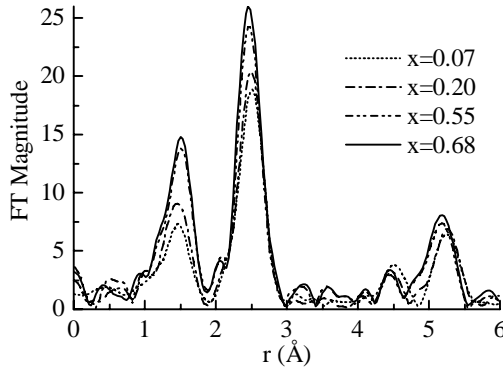


FIGURE 3. Fourier-transforms as a function of x for Ni in $\text{Li}_{1-x}\text{Ni}_{0.8}\text{Co}_{0.15}\text{Al}_{0.05}\text{O}_2$ (fresh cell, CEY-XAFS).

Fourier-transforms of the Ni K-edge EXAFS spectra for the fresh cell as a function of x in $\text{Li}_{1-x}\text{Ni}_{0.8}\text{Co}_{0.15}\text{Al}_{0.05}\text{O}_2$ are shown in Figure 3 (CEY-XAFS). The first peak at around 1.5 Å corresponds to Ni-O interaction and the second one at around 2.5 Å corresponds to Ni-M (M = Ni, Co) interaction. It can be seen that the amplitude of Ni-O peak increases with charging. The smaller amplitude before charging is well understood by considering the local Jahn-Teller effect of NiO_6 octahedron expected for Ni^{3+} in a low-spin state.

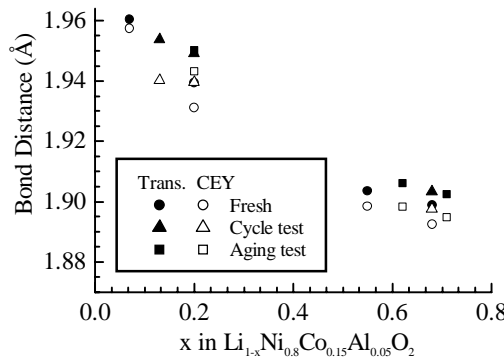


FIGURE 4. Variations of the average Ni-O bond lengths obtained by the fitting to the first peak of the Ni K-edge FT.

In Figure 4 are plotted Ni-O bond distances deduced from curve-fits as a function of x in $\text{Li}_{1-x}\text{Ni}_{0.8}\text{Co}_{0.15}\text{Al}_{0.05}\text{O}_2$. The Ni-O peak, which is actually composed of contributions from four subshells (one Ni^{2+} -O, two Ni^{3+} -Os and one Ni^{4+} -O) was fitted to one Ni-O shell. The bulk-averaged Ni-O

bond distance for the fresh cell decreases with increasing the value of x. This behavior is attributed to the conversion of Ni oxidation state from Ni^{3+} to Ni^{4+} . As described above the Ni^{3+} -O shell is composed of 4 shorter and 2 longer bonds, both of which are longer than the Ni^{4+} -O bond [7]. The bulk-averaged Ni-O bond distances for the cycle and aging tested cells behave very similarly to that for the fresh cell. This is surprising because the drops in Ni valences observed in XANES spectra for the tested cells are expected to result in expanding Ni-O bond distance due to larger Ni^{2+} ionic radius than Ni^{3+} one. More surprisingly, the surface-averaged Ni-O distances appear to be slightly shorter than the bulk-averaged one for all cell conditions. These distances are much shorter than a distance of 2.08 Å that is expected for the case of pure NiO . These observations mean that, in spite of the increase in the content rate of divalent Ni atom, the bulk and surface-averaged Ni-O bond distances remain unchanged after the cycle and aging tests, and the slight contraction of Ni-O distance occurs at the surface of the cathode materials for all cell conditions.

Our XANES results are in good agreement with the Abraham *et al.*'s observation for $\text{LiNi}_{0.8}\text{Co}_{0.2}\text{O}_2$ [8]. Their TEM and electron energy loss spectroscopy (EELS) data showed that the Ni-O like surface layer having NaCl-type structure was existent at the surface of the cathode material particles and it grew during the aging test. They proposed a possible mechanism of the capacity fading; the presence of Ni-O like layer which may reduces electronic and ionic conductivities is the main reason for the capacity fading. We support their proposition and believe that the similar phenomena occur also in the case of $\text{LiNi}_{0.8}\text{Co}_{0.15}\text{Al}_{0.05}\text{O}_2$.

REFERENCES

1. H. Cao, B. Xia, N. Xu, C. Zhang, *J. Alloys Compd.*, **376**, 282-286 (2004).
2. Y. Itou, Y. Ukyo, *J. Power Sources*, **146**, 39-44 (2005).
3. K. Amine, C.H. Chen, J. Liu, M. Hammond, A. Jansen, D. Dees, I. Bloom, D. Vissers, G. Henriksen, *J. Power Sources*, **97-98**, 684-687 (2001).
4. M. Takahashi, M. Harada, I. Watanabe, T. Uruga, H. Tanida, Y. Yoneda, S. Emura, T. Tanaka, H. Kimura, Y. Kubozono, S. Kikkawa, *J. Synchrotron Rad.*, **6**, 222-224 (1999).
5. S.L.M. Schroeder, G.D. Mogridge, R.M. Ormerod, T. Rayment, R.M. Lambert, *Surf. Sci. Lett.*, **324**, 371-377 (1995).
6. W.E. O'Grady, K.I. Pandya, K.E. Swider, D.A. Corrigan, *J. Electrochem. Soc.*, **143**, 1613-1617 (1996).
7. M. Balasubramanian, X. Sun, X.Q. Yang, J. McBreen, *J. Electrochem. Soc.*, **147**, 2903-2909 (2000).
8. D.P. Abraham, R.D. Tweten, M. Balasubramanian, J. Kropf, D. Fischer, J. McBreen, I. Petrov, K. Amine, *J. Electrochem. Soc.*, **150**, 1450-1456 (2003).